


**AUTHOR QUERY FORM**

 ELSEVIER	<b>Journal: YNIMG</b>  <b>Article Number: 8478</b>	<b>Please e-mail or fax your responses and any corrections to:</b> <b>E-mail: <a href="mailto:corrections.essd@elsevier.spitech.com">corrections.essd@elsevier.spitech.com</a></b> <b>Fax: +1 619 699 6721</b>
---	--	--

Dear Author,

Any queries or remarks that have arisen during the processing of your manuscript are listed below and highlighted by flags in the proof. Please check your proof carefully and mark all corrections at the appropriate place in the proof (e.g., by using on-screen annotation in the PDF file) or compile them in a separate list.

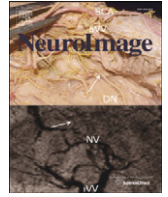
For correction or revision of any artwork, please consult <http://www.elsevier.com/artworkinstructions>.

No queries have arisen during the processing of your article.

Thank you for your assistance.

Contents lists available at [ScienceDirect](#)

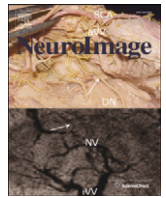
NeuroImage

journal homepage: [www.elsevier.com/locate/ynimg](http://www.elsevier.com/locate/ynimg)

## Highlights

**A linear model for estimation of neurotransmitter response profiles from dynamic PET data***NeuroImage xxx (2011) xxx–xxx*M.D. Normandin <sup>a,b</sup>, W.K. Schiffer <sup>c</sup>, E.D. Morris <sup>a,b,d,\*</sup><sup>a</sup> Weldon School of Biomedical Engineering, Purdue University, West Lafayette, IN, USA<sup>b</sup> Department of Radiology, Indiana University School of Medicine, Indianapolis, IN, USA<sup>c</sup> Medical Department, Brookhaven National Laboratory, Upton, NY, USA<sup>d</sup> Department of Biomedical Engineering, Indiana University-Purdue University at Indianapolis, Indianapolis, IN, USA

- ▶ A basis function model estimates neurotransmitter kinetics from PET data. ▶ Estimated neurotransmitter profiles have temporal precision of ~3 min. ▶ The model can analyze single-scan data and is insensitive to model violations. ▶ Dopamine responses estimated from rats agree with simultaneous microdialysis.
- ▶ Performance is similar to an alternative method, but orders of magnitude faster.



# A linear model for estimation of neurotransmitter response profiles from dynamic PET data

M.D. Normandin<sup>a,b,1</sup>, W.K. Schiffer<sup>c,2</sup>, E.D. Morris<sup>a,b,d,\*</sup>

<sup>a</sup> Weldon School of Biomedical Engineering, Purdue University, West Lafayette, IN, USA

<sup>b</sup> Department of Radiology, Indiana University School of Medicine, Indianapolis, IN, USA

<sup>c</sup> Medical Department, Brookhaven National Laboratory, Upton, NY, USA

<sup>d</sup> Department of Biomedical Engineering, Indiana University-Purdue University at Indianapolis, Indianapolis, IN, USA

## ARTICLE INFO

### Article history:

Received 10 February 2011

Revised 26 May 2011

Accepted 1 July 2011

Available online xxxx

### Keywords:

Basis functions

Compartmental modeling

Dopamine

Neurotransmitter

PET

Reference region

Tracer kinetics

## ABSTRACT

The parametric ntPET model (p-ntPET) estimates the kinetics of neurotransmitter release from dynamic PET data with receptor-ligand radiotracers. Here we introduce a linearization (lp-ntPET) that is computationally efficient and can be applied to single scan data. lp-ntPET employs a non-invasive reference region input function and extends the LSRRM of Alpert et al. (2003) using basis functions to characterize the time course of neurotransmitter activation. In simulation studies, the temporal precision of neurotransmitter profiles estimated by lp-ntPET was similar to that of p-ntPET (standard deviation ~3 min for responses early in the scan) while computation time was reduced by several orders of magnitude. Violations of model assumptions such as activation-induced changes in regional blood flow or specific binding in the reference tissue have negligible effects on lp-ntPET performance. Application of the lp-ntPET method is demonstrated on [<sup>11</sup>C] raclopride data acquired in rats receiving methamphetamine, which yielded estimated response functions that were in good agreement with simultaneous microdialysis measurements of extracellular dopamine concentration. These results demonstrate that lp-ntPET is a computationally efficient, linear variant of ntPET that can be applied to PET data from single or multiple scan designs to estimate the time course of neurotransmitter activation.

© 2011 Published by Elsevier Inc. 40

## Introduction

Neurotransmission is central to synaptic signaling in the brain. Acute fluctuations of specific neurotransmitters have been demonstrated in normal motor and cognitive function (Aalto et al., 2005; Badgaiyan et al., 2003; Christian et al., 2006; Koeppe et al., 1998), whereas dysregulation of phasic release has been implicated in schizophrenia (Abi-Dargham et al., 1998; Breier et al., 1997; Laruelle et al., 1999), substance abuse (Busto et al., 2009; Cox et al., 2009; Martinez et al., 2005, 2007; Volkow et al., 1997), stress (Oswald et al., 2005, 2007; Wand et al., 2007), and subpopulations of Parkinson's disease patients (de la Fuente-Fernández et al., 2004; Evans et al., 2006; Steeves et al., 2009). Investigators have postulated that the magnitude and temporal kinetics of changes in

neurotransmitter concentration represent distinct aspects of the response with differential implications in health, disease, and treatment (Fried et al., 2001; Olive et al., 2002; Parasrampur et al., 2007; Spencer et al., 2006; Volkow and Swanson, 2003; Volkow et al., 1995, 1996, 1999, 2002).

PET and SPECT have been applied to image neurotransmitter release using receptor-ligand tracers whose binding is sensitive to the concentration of endogenous neurotransmitter. Data are often analyzed using change in binding potential ( $\Delta BP_{ND}$ ; Innis et al., 2007), which reflects an alteration in the number of available receptors between baseline and activation scan conditions. It has been shown that the timing and magnitude of neurotransmitter release are conflated in measures of  $\Delta BP_{ND}$  (Endres and Carson, 1998; Yoder et al., 2004). More sophisticated experiment designs and data analysis techniques have been described (Alpert et al., 2003; Aston et al., 2000; Friston et al., 1997; Ikoma et al., 2009; Pappata et al., 2002; Watabe et al., 2000; Zhou et al., 2006), but these methods either fail to incorporate the dynamic nature of neurotransmitter release or else prescribe the temporal kinetics *a priori*. Hence these approaches focus on the detection of neurotransmitter release rather than its characterization. It has been suggested that the limited temporal information extracted from *in vivo* molecular imaging studies has yielded results – and consequently, new hypotheses – that emphasize

\* Corresponding author at: Yale PET Center, P.O. Box 208048, New Haven, CT 06520, USA.

E-mail address: [evan.morris@yale.edu](mailto:evan.morris@yale.edu) (E.D. Morris).

<sup>1</sup> Present address: Harvard Medical School and the Massachusetts General Hospital, Division of Nuclear Medicine and Molecular Imaging, Boston, MA, USA.

<sup>2</sup> Present address: Feinstein Institute for Medical Research, North Shore-Long Island Jewish Health System, Manhasset, NY, USA.

<sup>3</sup> Present address: Department of Diagnostic Radiology, School of Medicine, Yale University, New Haven, CT, USA.

static aberrations and discount dynamic dysregulation of neurotransmission which may underly certain disease phenotypes (Sarter et al., 2007).

To address the limitations of existing methodologies, we have developed data analysis techniques collectively termed ntPET (for ‘neurotransmitter PET’) which estimate the time course of neurotransmitter release from dynamic PET data with displaceable radiotracers. We have previously described two variants, one that is model-based or “parametric” (p-ntPET; Morris et al., 2005) and another that is data-driven or “non-parametric” (np-ntPET; Constantinescu et al., 2007). Estimating the eleven parameters of the p-ntPET model is computationally intensive. The model-independent np-ntPET method can recover response patterns of arbitrary shape and analyze data more rapidly. However, without an underlying model structure the solutions provided by this method can be more difficult to interpret or constrain to a particular form. Both p-ntPET and np-ntPET require data from two PET sessions, one at the baseline condition and the other during activation (i.e., neurotransmitter-releasing challenge). Analysis methods which require only one scan session (e.g., Alpert et al., 2003; Carson et al., 1997; Endres et al., 1997; Friston et al., 1997; Ikoma et al., 2009; Pappata et al., 2002; Zhou et al., 2006) are desirable to minimize cost, radiation dose, and physiological variation.

Thus, we seek an ntPET method that is computationally efficient and can be applied to data from a single scan session. Here, we extend the LSRRM analysis technique (Alpert et al., 2003) using a basis function approach to obtain a new model-based variant of ntPET, which we call lp-ntPET (‘linear parametric ntPET’). By analyzing realistic simulated data we show that the lp-ntPET method performs similarly to p-ntPET, is computationally efficient, is insensitive to plausible violations of model assumptions, and can be used to analyze data from experiments with single or paired scan sessions. We also demonstrate application of the technique to analyze [<sup>11</sup>C]raclopride data acquired in rats with a dopamine-releasing pharmacological challenge and compare the estimated response profiles to extracellular dopamine concentration measured simultaneously by microdialysis.

**Materials and methods**

*Theory*

The lp-ntPET model extends the LSRRM (Alpert et al., 2003) using basis functions to estimate the time course of neurotransmitter activation. The LSRRM is, in turn, a linear extension of the simplified reference tissue model (SRTM; Lammertsma and Hume, 1996). Integration of the SRTM equations yields a formulation that is linear in its parameters,

$$C_T(t) = R_1 C_R(t) + k_2 \int_0^t C_R(u) du - k_{2a} \int_0^t C_T(u) du \tag{1}$$

where  $C_T$  and  $C_R$  are concentration of tracer in the target and reference regions, respectively, and the coefficients describe the kinetics of tracer uptake and retention in the tissue. (This integral expression was derived independently by Ichise et al. (2003) and termed the multilinear reference tissue model, or MRTM.) Alpert et al. generalized this model with time-varying parameters that reflect transient changes in radiotracer influx, clearance, and binding. The fluctuations of the parameters during the activation state were described by the time course of the function  $h(t)$ ,

$$C_T(t) = R_1 C_R(t) + \alpha \int_0^t \frac{dC_R}{du} h(u) du + k_2 \int_0^t C_R(u) du + \beta \int_0^t C_R(u) h(u) du - k_{2a} \int_0^t C_T(u) du - \gamma \int_0^t C_T(t) h(u) du. \tag{2}$$

Extending the logic applied previously for exogenous pharmacological competition with a radioligand (Friston et al., 1997) Alpert recognized that  $k_{2a}$ , the tracer efflux rate from the collapsed tissue compartment to plasma, was sensitive to radiotracer displacement caused by endogenous neurotransmitter release. The effect of neurotransmission being of primary interest, the impact of changes in tracer delivery and clearance were evaluated separately with a reduced model having one time-varying parameter  $k_{2a}(t)$  of the form  $k_{2a} + \gamma h(t)$ , where  $k_{2a}$  is the baseline washout rate constant,  $h(t)$  represents the time course of activation and  $\gamma$  encodes the magnitude of its effect on the apparent tissue efflux rate. Provided  $h(t)$  is defined in advance, the model can still be expressed in terms of linear parameters:

$$C_T(t) = R_1 C_R(t) + k_2 \int_0^t C_R(u) du - k_{2a} \int_0^t C_T(u) du - \gamma \int_0^t C_T(u) h(u) du. \tag{3}$$

Alpert et al. set  $h(t) = e^{-\tau(t-T)} u(t-T)$  where  $u(t)$  is the unit step function and  $T$  is the time at which the activation is initiated, an expression used previously by Endres and Carson (1998) to model dopamine release elicited by intravenous administration of amphetamine. This mathematical formulation applies to a neurotransmitter response that becomes maximal instantaneously at the onset of the challenge and decays exponentially to baseline thereafter. With the temporal qualities of the response predetermined, applications of LSRRM (Badgaiyan et al., 2003, 2007, 2008; Christian et al., 2006) have focused on detection of neurotransmitter release by testing whether  $\gamma$ , the response magnitude, was statistically different than zero.

We have extended LSRRM using a basis function approach for the dual purposes of detection and characterization of neurotransmitter responses that may have greater complexity than a single exponential functions. We refer to this model as linear parametric ntPET (lp-ntPET). The basis functions are of the form

$$B_i(t) = \int_0^t C_T(u) h_i(u) du \tag{4}$$

where the constituent functions,  $h_i(t)$ , comprise a predefined catalog of candidate response profiles. Because each basis function is constructed from the same measured time activity curve,  $C_T(t)$ , every  $B_i(t)$  is affiliated with a unique response function. The operational equation for lp-ntPET is

$$C_T(t) = R_1 C_R(t) + k_2 \int_0^t C_R(u) du - k_{2a} \int_0^t C_T(u) du - \gamma B_i(t). \tag{5}$$

This relationship can be expressed compactly in standard matrix notation of the form  $y = Ax$ . The corresponding linear algebraic equation for analysis of single-scan data is

$$\begin{bmatrix} C_T(t_1) \\ \vdots \\ C_T(t_m) \end{bmatrix} = \begin{bmatrix} C_R(t_1) & \int_0^{t_1} C_R(u) du & -\int_0^{t_1} C_T(u) du & -\int_0^{t_1} C_T(u) h_i(u) du \\ \vdots & \vdots & \vdots & \vdots \\ C_R(t_m) & \int_0^{t_m} C_R(u) du & -\int_0^{t_m} C_T(u) du & -\int_0^{t_m} C_T(u) h_i(u) du \end{bmatrix} \times \begin{bmatrix} R_1 \\ k_2 \\ k_{2a} \\ \gamma \end{bmatrix}. \tag{6}$$

179 For analysis of dual-scan data the relevant formula is

$$\begin{bmatrix} C_T^b(t_1) \\ \vdots \\ C_T^b(t_m) \\ C_T^a(t_1) \\ \vdots \\ C_T^a(t_n) \end{bmatrix} = \begin{bmatrix} C_R^b(t_1) & \int_0^{t_1} C_R^b(u)du & -\int_0^{t_1} C_T^b(u)du & 0 \\ \vdots & \vdots & \vdots & \vdots \\ C_R^b(t_m) & \int_0^{t_m} C_R^b(u)du & -\int_0^{t_m} C_T^b(u)du & 0 \\ C_R^a(t_1) & \int_0^{t_1} C_R^a(u)du & -\int_0^{t_1} C_T^a(u)du & -\int_0^{t_1} C_T^a(u)h_i(u)du \\ \vdots & \vdots & \vdots & \vdots \\ C_R^a(t_n) & \int_0^{t_n} C_R^a(u)du & -\int_0^{t_n} C_T^a(u)du & -\int_0^{t_n} C_T^a(u)h_i(u)du \end{bmatrix} \times \begin{bmatrix} R_1 \\ k_2 \\ k_{2a} \\ \gamma \end{bmatrix} \quad (7)$$

180 where the superscripts *a* and *b* designate PET data from activation and  
 182 baseline sessions, respectively.

183 For each basis function the overdetermined system of equations can  
 184 be solved rapidly using standard algorithms to obtain the weighted least  
 185 squares estimate of model parameters  $\hat{x} = (A^TWA)^{-1}A^TWy$ , where **W**  
 186 is the weighting matrix having diagonal elements inversely propor-  
 187 tional to the variance of the PET measurement  $C_T$  contained in the  
 188 matching row of the matrix equation. The optimal model parameters  
 189 and activation pattern are identified from the basis function that yields  
 190 the best model fit to the data. This approach is not unlike the basis  
 191 function implementation of SRTM (Gunn et al., 1997). However, instead  
 192 of constructing basis functions that map to different binding potential  
 193 values (the *parameter* of interest in SRTM), we employ basis functions  
 194 that map to distinct neurotransmitter response curves (the *vector* of  
 195 interest in lp-ntPET).

196 In the same manner that Gunn et al. (1997) created basis functions by  
 197 discretizing the direct search parameter over a physiologically relevant  
 198 range, the curves included in the family  $h_i(t)$  were chosen to restrict  
 199 the search to plausible response functions. As was done previously with  
 200 p-ntPET, the response profiles were parameterized by gamma variate  
 201 functions. Here, we have used the formulation of Madsen (1992),

$$h_i(t) = \left(\frac{t-t_D}{t_p-t_D}\right)^\alpha \exp\left(\alpha\left[1-\frac{t-t_D}{t_p-t_D}\right]\right)u(t-t_D) \quad (8)$$

202 where  $u(t)$  is the unit step function and the variables  $t_D$  (the delay  
 204 time at which the response starts relative to start of scan),  $t_p$  (the peak  
 205 time of maximal response magnitude), and  $\alpha$  (the “sharpness” of the  
 206 function) are incremented over finite intervals. Here we used the  
 207 following values to discretize the parameters, where  $t_{end}$  designates  
 208 the time at which the scan ended:  $\alpha$  equal 0.25, 1, or 4;  $t_D$  equal  $-5$  to

( $t_{end} - 10$ ) in increments of 2.5 min;  $t_p$  equal ( $t_D + 1.25$ ) to ( $t_{end} - 5$ )  
 in increments of 2.5 min. Note that the lower limit of  $t_p$  is conditioned  
 on the value of  $t_D$  as it is not sensible for a response to peak before it  
 begins, and the limits of both  $t_D$  and  $t_p$  are restricted so that only  
 responses which occur during the PET session are evaluated. The  
 permutations of the discretized parameter values yield at total of 897  
 distinct functions.

A subset of the functions included in the response catalog is  
 plotted in Fig. 1A for a fixed onset time. These functions have a variety  
 of shapes and peak times, and resemble neurotransmitter time  
 courses that we might anticipate in response to drug administration  
 or a behavioral task. We note that the model could readily  
 accommodate curves of any arbitrary form if additional information  
 were available to guide the choice of response profiles. Fig. 1B depicts  
 the basis functions generated according to Eq. (4) using the subset of  
 response functions and a noiseless simulated tissue curve. Note from  
 the operational Eq. (5) that the basis functions represent the  
 sensitivity curves  $dC_T(t)/d\gamma$  for each  $h_i(t)$ , and their distinct shapes  
 distinguish one from another during the optimization process.

The lp-ntPET model has four explicit parameters ( $R_1, k_2, k_{2a}, \gamma$ ) that  
 describe tracer kinetics and response magnitude, and three implicit  
 parameters encoded by the basis functions ( $t_D, t_p, \alpha$ ) that describe the  
 time course of the response. This formulation represents a simplifi-  
 cation of p-ntPET which relies on the eleven-parameter enhanced  
 receptor model (Endres et al., 1997; Morris et al., 1995) which is an  
 extension of the two-tissue compartment model (Mintun et al., 1984)  
 that explicitly accounts for competition between the tracer and the  
 endogenous neurotransmitter at the receptor sites.

237 *Simulated PET data*

238 *Dual-scan data*

Realistic simulated PET data with kinetics chosen to resemble [<sup>11</sup>C]  
 raclopride were generated as previously described (Normandin and  
 Morris, 2008). Briefly, three types of noisy data sets were created: (i)  
 data without model violations, (ii) data with imperfect reference  
 regions biased by specific binding, and (iii) data with activation-  
 induced changes in blood flow. As in Normandin and Morris (2008),  
 changes in regional blood flow were simulated by 10% changes in  $K_1$   
 and  $k_2$  starting at the time of activation onset and lasting through the  
 end of the scan. In the target region the parameters were increased  
 and in the reference region were constant or decreased, in order to  
 mimic changes in blood flow previously observed after ethanol  
 administration (Volkow et al., 1988). Each simulated data set  
 consisted of four time activity curves (TACs), corresponding to target  
 and reference region curves during baseline and activation sessions.  
 All cases were replicated for neurotransmitter responses commencing  
 between 0 and 45 minutes in 5 minute increments, the only exception

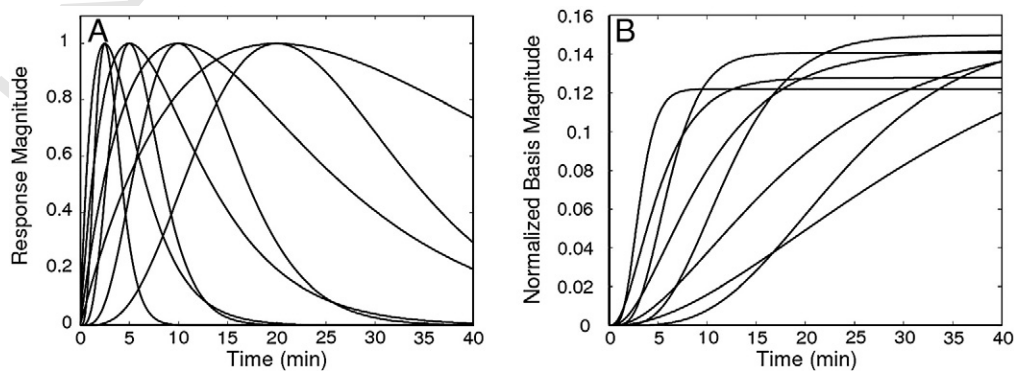


**Fig. 1.** Example response and basis functions. (A) Family of activation responses and (B) basis functions generated from them. To aid visualization, a small subset of functions is displayed and the basis functions are normalized by the integral of the corresponding response function in order to yield bases of a similar scale. Also note that the response curves in this subset all have the same onset time ( $t = 0$ ), whereas the entire set of functions includes profiles with a variety of start times.



being data with changes in blood flow for which activation always occurred at 15 minutes. Each neurotransmitter response peaked 10 minutes after take-off. “Null” data sets also consisted of four TACs, but neurotransmitter levels were constant during both rest and activation conditions. For each case at a given response start time, 1000 data sets with unique random noise realizations were generated. This approach parallels the tests performed to characterize p-ntPET with reference region-derived input functions (Normandin and Morris, 2008).

It should be noted that lp-ntPET relies on a simplification of the two-tissue compartment model that collapses the free and bound tracer states into a single compartment, but the simulated data were generated using the complete enhanced receptor model (Endres et al., 1997; Morris et al., 1995) with parameters derived from experimental data. Furthermore, none of the response functions in the  $h_i(t)$  catalog shared the same temporal profile as the neurotransmitter concentration curve used to generate simulated data with the enhanced receptor model.

### Single-scan data

Data were created in the same manner as for dual-scan sets as described above, but only TACs from the activation scan were generated and analyzed. All curves were noisy but unbiased. The impact of specific binding in the reference tissue or alteration of blood flow parameters was not assessed for the single-scan paradigm.

### Parameter estimation

#### Optimization algorithms

The lp-ntPET model was fitted to data using linear least squares estimation. Two optimization variants were evaluated. Weighted least squares (WLS) was applied with each weighting factor set inversely proportional to the variance of the corresponding target region PET datum, as is customary in PET analysis (Landaw and DiStefano, 1984; Mazoyer et al., 1986). The WLS solution is unique and can be obtained efficiently using standard algorithms. Because WLS can estimate positive or negative values for gamma, response profiles reflecting increases or decreases in neurotransmitter level can be estimated. Non-negative least squares (NNLS) was also applied with residuals weighted in the same manner. The imposition of a non-negativity constraint necessitates iterative fitting and allows only positive response profiles to be estimated. In p-ntPET estimations reported previously (Normandin and Morris, 2006, 2008; Morris et al., 2005, 2008), we set a lower bound of zero for the scaling factor of the neurotransmitter profile. Therefore, lp-ntPET with NNLS most closely resembles the p-ntPET method.

#### Use of prior information to constrain fits

The response functions to be evaluated during estimation are chosen at the discretion of the investigator. If information were known about the experiment, for example when the challenge was initiated, one could incorporate that knowledge into the lp-ntPET framework through the exclusion of certain components in the response catalog (i.e., the set of functions  $h_i(t)$ ). For these simulation experiments we selected candidate functions in two ways: (i) using the full catalog of response functions without constraints on response start time, or (ii) by excluding responses starting more than five minutes before the true neurotransmitter response as a way of constraining responses based on prior information (e.g., the experimentally known challenge initiation time). We have previously applied p-ntPET with (Morris et al., 2008) or without (Normandin and Morris, 2006, 2008; Morris et al., 2005) constraints on time of response onset.

### Significance testing

Each data set was fitted with both MRTM (1) and lp-ntPET (5). MRTM is a nested model, identical to lp-ntPET absent the activation

term. The significance of the responses estimated by lp-ntPET was assessed using model selection criteria and statistical testing on  $\gamma$ , the estimated response magnitude.

For each data set a one-sample location test of the  $t$  statistic (Fisher, 1925a; Gosset [Student], 1908) was used to assess whether or not  $\gamma$  was statistically different than zero, indicative of a significant response. For a given fit, the  $t$  statistic is the ratio of the estimated parameter to its standard error. The parameter variance for an individual fit was obtained from the Fisher information matrix. This estimate of the variance is often called the Cramér–Rao lower bound (Cramér, 1946; Rao, 1945) and represents the minimum variance achievable by an unbiased estimator. Because the true parameter variance is generally greater than the Cramér–Rao bound, the  $t$  statistic calculated using this approximation may be artificially inflated. We therefore calculated “uncorrected”  $t$  values using the Cramér–Rao lower bound and “corrected”  $t$  values using a Monte Carlo-based estimate of the variance for  $\gamma$  as observed across the 1000 replicate data sets for each simulation case.

Alternatively, a likelihood ratio test was performed using the  $F$  statistic (Fisher, 1925b) to compare the goodness of fit of MRTM and lp-ntPET for each data set. Comparing two models where model 1 is nested within (i.e., is a degenerate form of) model 2, the  $F$  statistic is given by

$$F = \frac{\left( \frac{WRSS_1 - WRSS_2}{p_2 - p_1} \right)}{\left( \frac{WRSS_2}{n - p_2} \right)} \quad (9)$$

where WRSS is the weighted residual sum of squares,  $p$  is the number of model parameters,  $n$  is the number of data points, and the subscripts designate whether the quantity applies to model 1 or 2. In our application, model 1 is MRTM and model 2 is lp-ntPET. When only two models are considered and an unbiased estimator is used, the  $F$  statistic is equal to the square of the  $t$  statistic. In line with our treatment of the  $t$  statistic, we calculated the “uncorrected”  $F$  statistic according to (9) and the “corrected”  $F$  value normalized to reflect the difference between the Cramér–Rao lower bound and the variance determined by Monte Carlo estimation.

Similarly, the Akaike (AIC; Akaike, 1974) and Bayesian (BIC; Schwarz, 1978) information criteria were calculated for MRTM and lp-ntPET fits to each data set. The AIC is given by

$$AIC = n \log \left( \frac{WRSS}{n} \right) + 2p \quad (10)$$

and the BIC by

$$BIC = n \log \left( \frac{WRSS}{n} \right) + p \log(n). \quad (11)$$

The model with the lowest AIC or BIC is generally considered best. The structure of Akaike weights (Akaike, 1978; Burnham and Anderson, 1998) was used to assign a probability to a given model being best. Briefly, for each model we define  $\Delta_i = AIC_i - AIC_{\min}$ , where  $AIC_{\min}$  is the minimum AIC of all candidate models and the subscript  $i$  indexes the  $M$  candidate models. Here, we used  $M = 2$  to compare MRTM and lp-ntPET with the optimal basis function. For each model the Akaike weight is obtained by

$$w_i = \frac{\exp(-\Delta_i / 2)}{\sum_{j=1}^M \exp(-\Delta_j / 2)} \quad (12)$$

and represents the likelihood that the model is the best among those evaluated. The same procedure can be applied to derive probabilities from the calculated BIC values. In this manner, the AIC and BIC values

368 from MRTM and lp-ntPET fits to each data set were used to test  
369 whether the response estimated by lp-ntPET was significant.

370 For all of the above tests we considered lp-ntPET to have seven  
371 parameters. Although only four parameters ( $R_1$ ,  $k_2$ ,  $k_{2a}$ , and  $\gamma$ ) are  
372 explicitly estimated, the basis function search implicitly incorporates  
373 the response onset time ( $t_D$ ), peak time ( $t_P$ ), and sharpness ( $\alpha$ ) into  
374 the model.

### 375 Experimental PET data

376 Animal experiments were approved by the Brookhaven National  
377 Laboratory Institutional Animal Care and Use Committee. Dynamic  
378 PET and microdialysis were performed simultaneously as previously  
379 described (Morris et al., 2008). Briefly, dynamic PET data were  
380 acquired from rats using a microPET R4 scanner (Concorde Micro-  
381 systems, Inc., Knoxville, TN) after a bolus administration of [ $^{11}\text{C}$ ]  
382 raclopride. Microdialysis was performed simultaneously to assay  
383 extracellular dopamine concentration. During the PET acquisition,  
384 methamphetamine was infused unilaterally through the microdialysis  
385 probe into the right striatum. A control animal underwent the PET-  
386 microdialysis experiment but did not receive the drug.

387 PET images were reconstructed by Fourier rebinning followed by  
388 filtered backprojection. Time activity curves were extracted from  
389 regions of interest delineated on the left (untreated) and right  
390 (cannulated) striata, as well as the cerebellum. As was done

391 previously with p-ntPET (Morris et al., 2008), lp-ntPET was applied  
392 using the left striatal data as the rest condition and right striatal data  
393 as the activation condition. The cerebellum was used as the reference  
394 region.

## 395 Results

### 396 Analysis of simulated dual-scan data without model violations

#### 397 Unconstrained fitting

398 The characterization of neurotransmitter profiles by lp-ntPET was  
399 similar using either WLS or NNLS optimization. When prior  
400 information was not applied to constrain the timing of estimated  
401 profiles, the delay ( $t_D$ ) and peak ( $t_P$ ) time parameters estimated from  
402 data with neurotransmitter release starting before 25 min had small  
403 biases ( $<3$  min) and moderate standard deviations ( $\sigma = 3 - 6$  min).  
404 Fig. 2A shows the average response estimated using lp-ntPET with  
405 NNLS from 1000 data sets having responses starting at 10 min; Fig. 2D  
406 shows the same for data sets analyzed using WLS optimization.  
407 Although temporal resolution deteriorated for later activation, the  
408 estimated profiles still clearly resembled the true neurotransmitter  
409 curves as depicted in Figs. 2B, E for responses starting at 35 min.  
410 Timing parameters estimated from null data sets lacking a neuro-  
411 transmitter response were highly variable ( $\sigma = 20$  min) and the  
412 response profiles had no discernable pattern, as seen in Figs. 2C, F.

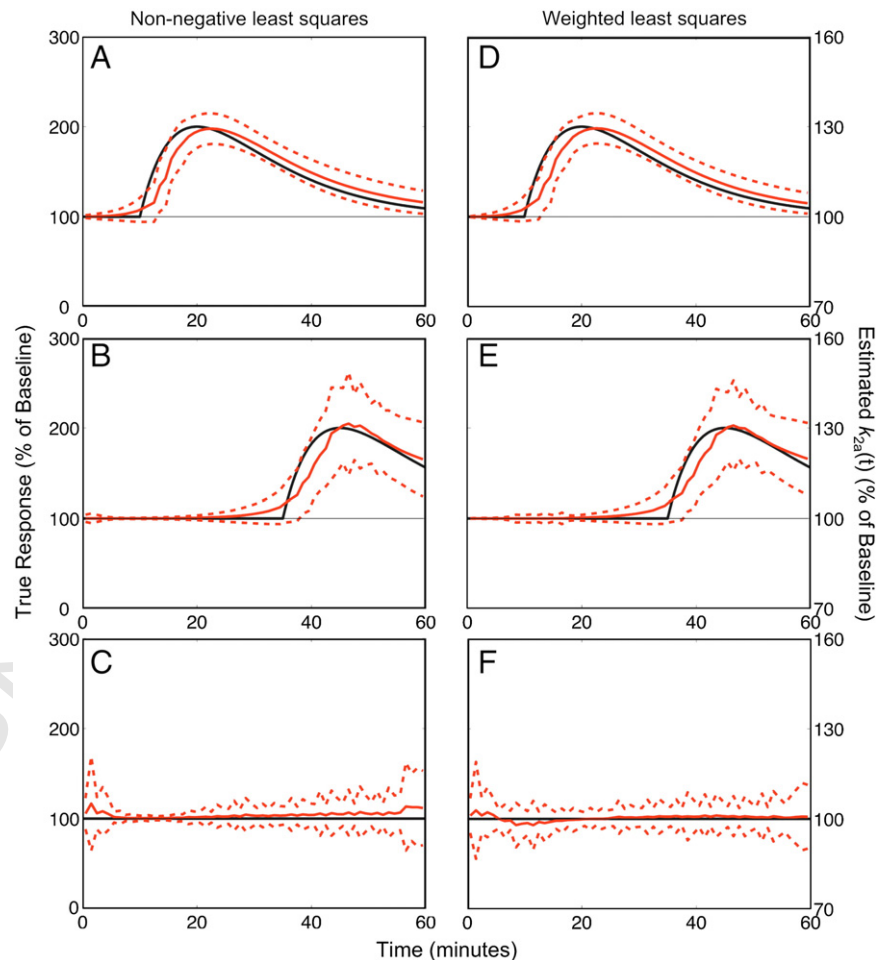


**Fig. 2.** Unconstrained fits of dual-scan data. Responses estimated using non-negative (NNLS; panels A–C) or weighted (WLS; panels D–F) least squares from dual-scan data with early (A, D), late (B, E), or no (C, F) NT response. Data were generated without model violations. Solid red curve: average of the estimated responses from 1000 simulated data sets expressed as percentage of the estimated baseline  $k_{2a}$ . Dashed red curves: envelope of  $\pm 1$  standard deviation about the mean. Black curve: true neurotransmitter response. Agreement between true and estimated responses for late activation is good, but degraded compared to data sets with early activation. Responses estimated from null data sets lacking activation are temporally incoherent with the zero magnitude level enclosed within the  $\pm 1$  s.d. interval. (For interpretation of the references to colour in this figure legend, the reader is referred to the web of this article.)

**Table 1**  
Bias and precision of estimated timing parameters.

			Single-scan	Dual-scan	Dual-scan (non-ideal ref. region)	Dual-scan (task-induced change in blood flow)	
$t_D = 15$ min	WLS	$t_D$	-1.26 (3.53)	0.77 (3.48)	-0.20 (3.49)	0.65 (3.41)	
		$t_P$	1.23 (2.72)	2.01 (3.19)	2.14 (3.20)	1.69 (3.04)	
		NNLS	$t_D$	-1.78 (3.53)	1.17 (3.52)	-0.01 (3.54)	1.09 (3.39)
			$t_P$	1.43 (2.70)	1.93 (3.21)	2.12 (3.50)	1.58 (3.14)
$t_D = 35$ min	WLS	$t_D$	-0.70 (4.23)	0.46 (4.65)	0.43 (4.96)	N/A	
		$t_P$	4.00 (6.62)	4.02 (6.43)	4.92 (6.63)	N/A	
	NNLS	$t_D$	-0.69 (4.33)	0.75 (4.76)	0.97 (5.16)	N/A	
		$t_P$	3.97 (6.55)	4.03 (6.05)	4.87 (6.22)	N/A	

Bias and standard deviation (in parentheses) of delay and peak time estimates across 1000 simulated data sets, in units of minutes. N/A: not applicable.

### Constrained fitting

Incorporation of prior information improved the accuracy and precision of neurotransmitter timing parameters. Performance was best for responses starting before 25 min, with small biases ( $\leq 2$  min) and standard deviations ( $\sigma = 3 - 4$  min) in estimates of both  $t_D$  and  $t_P$ . Bias of delay time remained stable for responses occurring throughout the scan duration whereas precision degraded slightly as true response delay time increased, reaching  $\sigma = 5$  min at  $t_D = 45$  min. Later activations led to slightly larger biases (up to  $\sim 4.5$  min) and variability ( $\sigma$  up to  $\sim 6.5$  min) in  $t_P$ . The biases and standard deviations of timing parameters for neurotransmitter responses starting at 15 or 35 min are reported in Table 1. Average responses estimated from data with activation at 35 min are shown in Fig. 3A. Analyses of null data yielded responses that lacked temporal coherence, as shown in Fig. 3B for challenge without neurotransmitter release at 35 min (that is, null data analyzed with constraint  $t_D \geq 30$  min). Throughout the remainder of this manuscript we report results from the application of lp-ntPET with constrained timing parameters unless otherwise noted.

True and false positive classification rates for activation at 15 and 35 min are given in Table 2. All significance tests consistently detected true neurotransmitter responses early in the scan using either NNLS or WLS estimation. Model selection criteria (AIC and BIC) and “uncorrected” statistical tests indicated strong significance for activations having start times ranging throughout most of the scan duration.

“Corrected” statistical tests ( $t$  and  $F$  values modified to reflect the observed variance of  $\gamma$  using Monte Carlo-based estimates) consistently designated the estimated responses as significant for early activation. Responses starting later than 25 min were detected with lower sensitivity. False positive rates estimated from null data were high for model selection criteria and uncorrected statistical tests, particularly for data with early responses analyzed using the WLS optimization algorithm. Corrected  $t$  and  $F$  tests generally had better specificity when WLS was used. False discovery rates from corrected  $t$  tests remained high with NNLS estimation.

### Analysis of simulated dual-scan data with non-ideal reference region

The presence of receptors in the reference region had little impact on the performance of lp-ntPET. Estimation of timing parameters was largely insensitive to specific binding in the reference region. Using a non-ideal reference tissue having receptor density equal to 40% of that in the target region, biases and standard deviations of the timing parameters were typically within one minute of those from unbiased data (refer to Table 1). Table 2 highlights classification results obtained using the same biased (reference region) input function. Performance was very similar to the case with an ideal reference region.

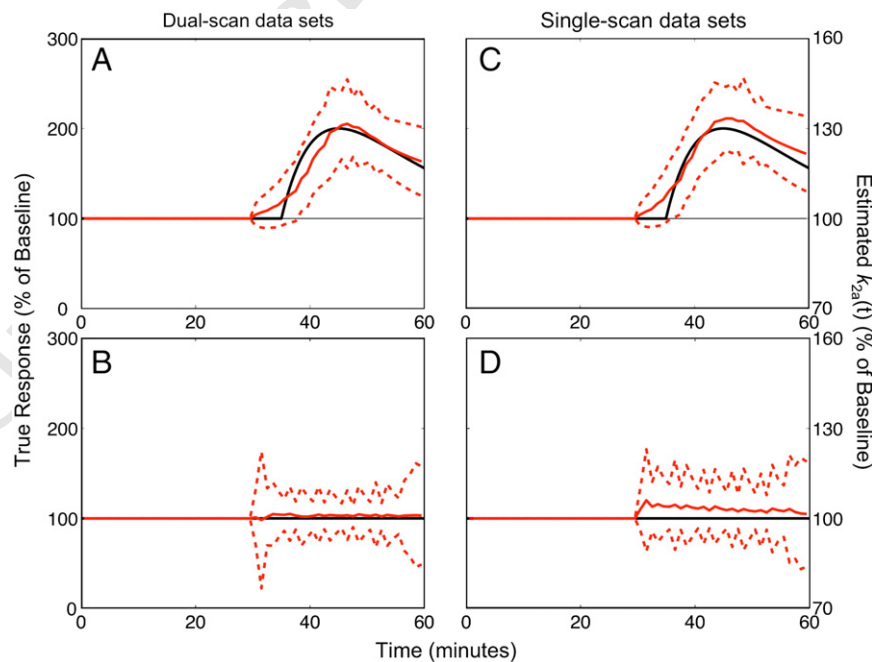


**Fig. 3.** Constrained fits of single- and dual-scan data. Comparison of responses estimated by lp-ntPET with WLS from dual-scan (A,B) or single-scan (C,D) data sets for late activation task. Data in upper panels include neurotransmitter release, while those in lower panels are null data sets. Responses were constrained to begin no earlier than 5 minutes before the challenge initiation. Results are presented as described in Fig. 2. Note the strong correspondence between true and estimated responses, and between the performance of the model applied to dual-scan versus single-scan data sets.



t2.1 **Table 2**  
Sensitivity and specificity of neurotransmitter response detection.

t2.2	t2.3			single-scan	dual-scan	dual-scan (biased input)	dual-scan (task-induced change in blood flow)
t2.4	t <sub>D</sub> = 15 min	WLS	AIC	0.99 (0.11)	1.00 (0.38)	1.00 (0.38)	1.00 (0.41)
t2.5			BIC	0.93 (0.02)	1.00 (0.22)	1.00 (0.20)	1.00 (0.23)
t2.6			t <sub>CR</sub>	1.00 (0.73)	1.00 (0.76)	1.00 (0.77)	1.00 (0.78)
t2.7			t <sub>MC</sub>	0.50 (0.00)	1.00 (0.01)	1.00 (0.01)	1.00 (0.01)
t2.8		F <sub>CR</sub>	1.00 (0.17)	1.00 (0.45)	1.00 (0.46)	1.00 (0.48)	
t2.9		F <sub>MC</sub>	0.01 (0.00)	0.98 (0.00)	0.99 (0.00)	0.99 (0.00)	
t2.10		NNLS	AIC	0.99 (0.12)	1.00 (0.16)	1.00 (0.19)	1.00 (0.23)
t2.11			BIC	0.91 (0.02)	1.00 (0.08)	1.00 (0.10)	1.00 (0.12)
t2.12	t <sub>CR</sub>		1.00 (0.71)	1.00 (0.37)	1.00 (0.37)	1.00 (0.45)	
t2.13	t <sub>MC</sub>		0.89 (0.16)	1.00 (0.15)	1.00 (0.14)	1.00 (0.17)	
t2.14	F <sub>CR</sub>		0.99 (0.19)	1.00 (0.20)	1.00 (0.21)	1.00 (0.27)	
t2.15	F <sub>MC</sub>		0.25 (0.01)	0.98 (0.05)	1.00 (0.04)	0.99 (0.05)	
t2.16	t <sub>D</sub> = 35 min	WLS	AIC	1.00 (0.03)	1.00 (0.22)	1.00 (0.25)	N/A
t2.17			BIC	0.97 (0.01)	0.98 (0.10)	0.98 (0.11)	N/A
t2.18			t <sub>CR</sub>	1.00 (0.44)	1.00 (0.61)	1.00 (0.63)	N/A
t2.19			t <sub>MC</sub>	0.01 (0.00)	0.03 (0.01)	0.03 (0.01)	N/A
t2.20		F <sub>CR</sub>	1.00 (0.05)	1.00 (0.29)	1.00 (0.32)	N/A	
t2.21		F <sub>MC</sub>	0.00 (0.00)	0.00 (0.00)	0.00 (0.00)	N/A	
t2.22		NNL <sub>t<sub>MC</sub></sub> S	AIC	1.00 (0.03)	0.99 (0.13)	0.99 (0.11)	N/A
t2.23			BIC	0.97 (0.01)	0.97 (0.05)	0.97 (0.04)	N/A
t2.24			t <sub>CR</sub>	1.00 (0.36)	1.00 (0.33)	1.00 (0.27)	N/A
t2.25			t <sub>MC</sub>	0.01 (0.11)	0.04 (0.14)	0.01 (0.09)	N/A
t2.26	F <sub>CR</sub>		1.00 (0.05)	0.99 (0.17)	0.99 (0.10)	N/A	
t2.27	F <sub>MC</sub>		0.00 (0.01)	0.00 (0.04)	0.00 (0.02)	N/A	

t2.28 True and false (in parentheses) positive rates for response detection tests with  $\alpha = 0.01$ . AIC: Akaike information criterion. BIC: Bayesian information criterion. *t*: *t* test. *F*: *F* test. CR: parameter variance from Cramér-Rao bound. MC: parameter variance from Monte Carlo analysis.

458 *Analysis of simulated dual-scan data with change in blood flow during*  
459 *activation*

460 Activation-induced alteration of blood flow resembling changes  
461 elicited by ethanol administration had negligible impact on the  
462 performance of Ip-ntPET. The estimated responses shown in Fig. 4  
463 correspond to data having increased blood flow to the target region  
464 and decreased blood flow to the reference region during activation  
465 (based on [<sup>15</sup>O]water PET studies (Volkow et al., 1988)). These  
466 response profiles are nearly identical to those estimated from data  
467 without activation-induced alteration of blood flow. The biases and

precision of estimated timing parameters were insensitive to this  
468 model violation (Table 1). Sensitivity and specificity of response  
469 detection were similar to comparable simulation cases without blood  
470 flow changes, although false positive rates were elevated by  
471 approximately 50% with NNLS optimization (see Table 2).  
472

473 *Analysis of simulated single-scan data*

474 The temporal characteristics of responses extracted from single-  
475 scan data sets (i.e., without a separate baseline session) compared  
476 favorably to the profiles estimated from analogous dual-scan data

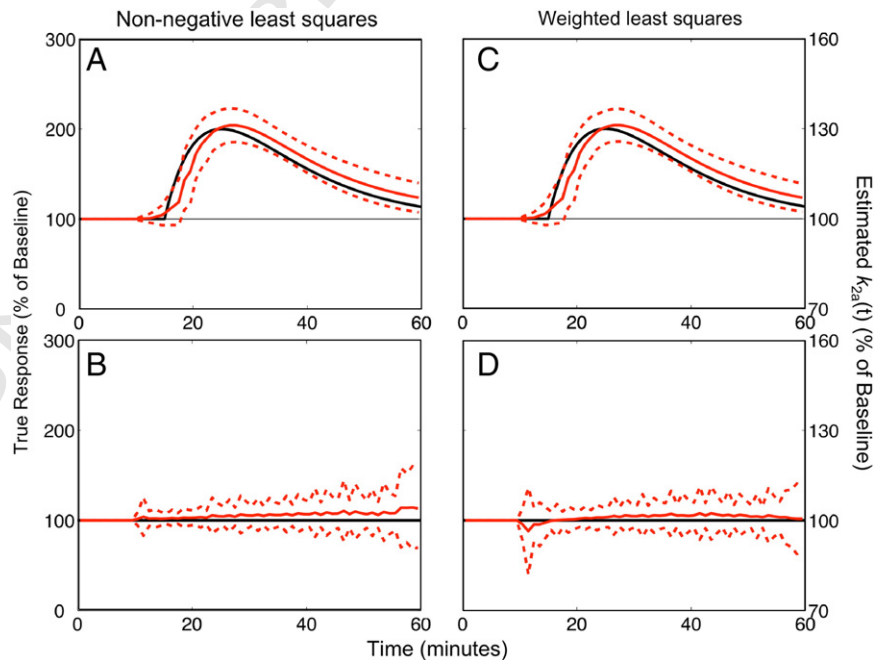


**Fig. 4.** Activation-induced change in blood flow. Responses estimated from dual-scan data with concomitant increased blood flow in the target region and decreased blood flow in reference region during activation. Data shown in upper panels include neurotransmitter release, while those in lower panels are null data sets. Results are presented as described in Fig. 2. Changes in blood flow had little impact on the performance of Ip-ntPET (compare to results in Fig. 2 and Table 1). Outcomes with decreased flow in the reference region (and no effect on the target region) were similar.

477 sets, as evidenced by the similarity of estimated responses shown in  
 478 Fig. 3 for dual- vs. single-scan data with activation at 35 min. Timing  
 479 parameters obtained from single-scan analyses were inaccurate and  
 480 inconsistent if responses occurred very early in the scan (before  
 481 15 min), but converged to performance as good as dual-scan analysis  
 482 for responses starting at 15–20 min or later (Table 1). Estimated  
 483 responses were consistently classified as significant across all  
 484 statistical tests for responses starting at 20–25 min, however the  
 485 sensitivity of corrected statistical tests diminished progressively  
 486 thereafter. Model selection tests exhibited better specificity with  
 487 single-scan analyses as compared to analogous dual-scan analyses  
 488 (Table 2).

#### 489 Analysis of experimental data

490 The activation profiles estimated by lp-ntPET with NNLS are  
 491 compared in Fig. 5 to the extracellular dopamine levels measured in  
 492 the striatum by microdialysis. Panels A–C show the measured data  
 493 and lp-ntPET results obtained from an animal that received  
 494 intracranial infusion of methamphetamine. The lp-ntPET fit was  
 495 statistically better than MRTM ( $p < 10^{-7}$  in all significance tests) and  
 496 yielded a response profile that was in good temporal agreement with  
 497 dopamine concentration measured by microdialysis (Fig. 5C). The  
 498 results obtained from a control animal that did not receive drug  
 499 treatment are shown in Figs. 5D–F. The response estimated by lp-  
 500 ntPET was not statistically significant ( $p > 0.98$  in all significance tests).  
 501 MRTM, which contains no neurotransmitter response term, provided  
 502 satisfactory fits when applied simultaneously to baseline and  
 503 sham data in the control experiment (Figs. 5D, E), but was unable  
 504 to reconcile the rest and activation data in the drug condition  
 505 (Figs. 5A, B).

#### Discussion

lp-ntPET was constructed as a basis function augmentation of the  
 linear extension of the simplified reference region model (LSRRM;  
 Alpert et al., 2003). LSRRM incorporated a temporal variation in  
 neurotransmission, which is absent from conventional analysis  
 techniques that typically estimate change in binding potential  
 ( $\Delta BP_{nd}$ ). However, the inclusion of temporal qualities was limited  
 because the model used a canonical response function. LSRRM was  
 introduced to address the binary question of whether or not the  
 prescribed response existed in the data. A noteworthy consequence of  
 this limitation was that the onset of the neurotransmitter response  
 needed to be known in advance and, in practice, was fixed to the time  
 of task initiation. The lp-ntPET model is free of this restriction and can  
 therefore estimate the full time course of neurotransmitter release.  
 Our analysis methods may also have alternative applications for  
 characterizing time-varying receptor occupancy by exogenous drugs.

#### Performance of lp-ntPET: Comparison to p-ntPET

The lp-ntPET model was devised to address the limitations of  
 LSRRM in order to provide a computationally efficient alternative to p-  
 ntPET. We have examined lp-ntPET using the same simulation tests  
 applied previously to characterize the reference region formulation of  
 the p-ntPET model (Normandin and Morris, 2008). When data were  
 noisy but without model violations, both p-ntPET and lp-ntPET  
 exhibited good precision in estimated timing parameters (standard  
 deviation approximately 3–4 min for neurotransmitter responses that  
 starting earlier than 25 min post-injection). p-ntPET was previously  
 tested on responses starting as late as 30 min, and a slight degradation  
 in its temporal precision was observed for later responses. Here,

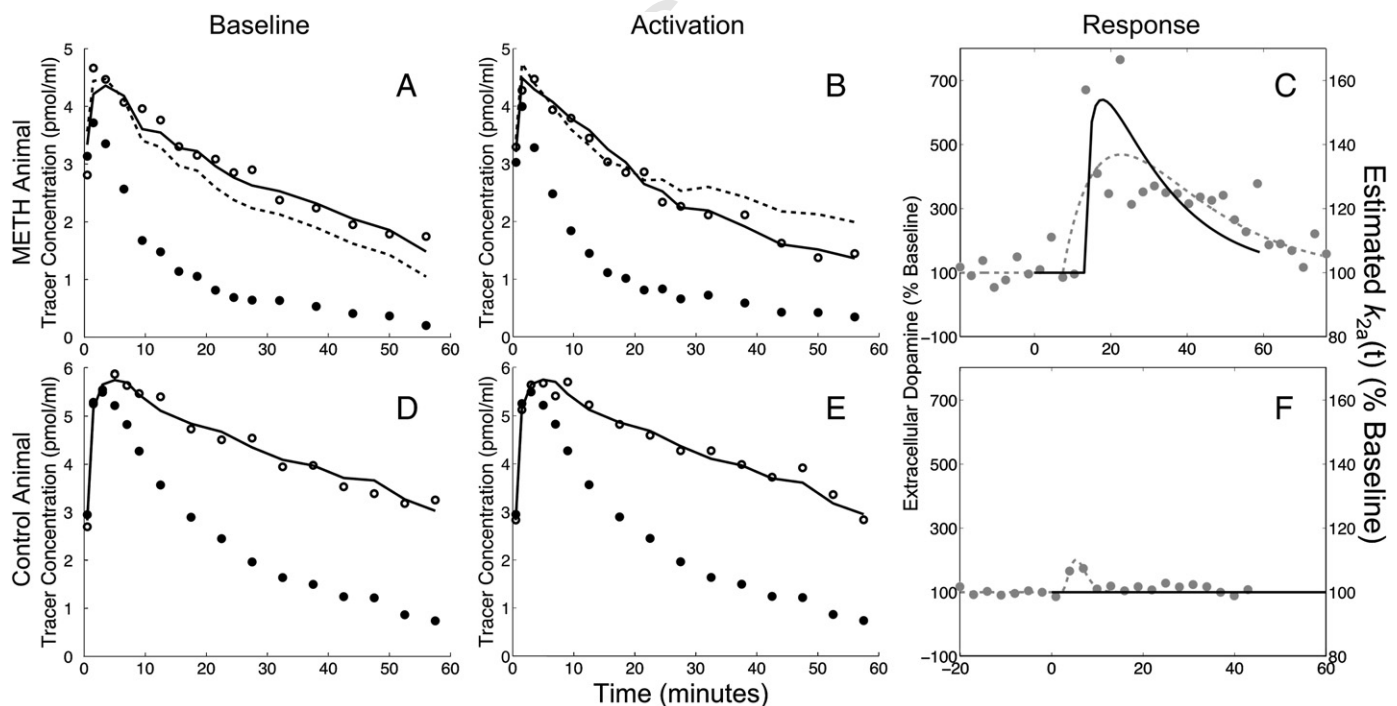


**Fig. 5.** Simultaneous PET-microdialysis experiments. Measured data and modeling results obtained from a rat that received intra-cranial infusion of methamphetamine (upper panels, A–C) and a control animal that received a sham infusion (lower panels, D–F). Baseline PET data from left striatum are shown in left panels (A, D) and activation data from right striatum are shown in middle column (B, E). Open circles: striatal PET data. Filled black circles: cerebellar PET data. Solid black curve: model fit obtained by lp-ntPET with WLS optimization. Dashed black curve: MRTM model fit. Neurotransmitter responses measured by microdialysis (left vertical axis) and estimated by lp-ntPET (right vertical axis) are plotted in the right panels (C, F). Filled gray circles: measured microdialysis data. Dashed gray curves: gamma variate function fitted to microdialysis data. Solid black curve: responses estimated by lp-ntPET. In the control animal, lp-ntPET and MRTM provide nearly identical fits (D, E); the response (F) estimated by lp-ntPET is not significant ( $p > 0.98$  in all tests). In the animal that received drug, the fit from the MRTM model (no activation term) is poor while lp-ntPET provides a good fit to the data (A, B); the response estimated by lp-ntPET is significant ( $p < 10^{-7}$  in all tests) and in good agreement with microdialysis measurements of dopamine (C).

534 lp-ntPET was evaluated using responses initiated as late as 45 min; a  
535 similar trend of reduced precision for later responses was observed.

536 p-ntPET and lp-ntPET exhibited comparable behavior when  
537 applied to data with model violations. The presence of receptors in  
538 the reference region, which biases the model input function, caused  
539 underestimation of binding potential but did not compromise the  
540 ability of either technique to estimate neurotransmitter timing  
541 parameters with accuracy and precision. This raises the possibility  
542 of using non-ideal reference tissues to improve the signal-to-noise  
543 properties of the input function if it can be assumed that neurotransmitter  
544 **fluctuations** in the reference region are negligible during the  
545 scan and accurate estimation of  $BP_{ND}$  is not required. These  
546 assumptions should be considered and appropriately validated on a  
547 case by case basis. The impact of changes in blood flow (alteration of  
548 both  $K_1$  and  $k_2$  coincident with activation) was also negligible for both  
549 methods. Changes in  $K_1$  alone were detrimental to the performance of  
550 both models, affecting sensitivity to neurotransmitter responses and  
551 obscuring their timing (data not shown). We note that changes in  $K_1$   
552 decoupled from changes in  $k_2$  are physiologically implausible for  
553 tracers whose transport between blood and tissue is governed by  
554 passive diffusion. If such effects did occur they would adversely affect  
555 conventional analysis methods as well, as shown previously for  $\Delta BP_{ND}$   
556 (Normandin and Morris, 2008).

#### 557 Constraints based on prior information

558 Although the structures of the p-ntPET and lp-ntPET models differ,  
559 analogous adaptations can be made to restrict parameters to fixed  
560 values or within reasonable bounds based on knowledge of  
561 physiology or experimental conditions. Prior information has been  
562 used in p-ntPET to constrain the peak time and baseline binding  
563 potential (Morris et al., 2008; Normandin and Morris, 2008). Said  
564 constraints were imposed via penalty functions, terms added to the  
565 objective function which promote solutions having particular quali-  
566 ties (e.g., responses that peak during scan period). We can also  
567 incorporate prior information into the optimization of lp-ntPET. For  
568 instance, the member functions  $h_i(t)$  of the response catalog were  
569 chosen to exclude responses whose maximum **occurred** after the end  
570 of the scan. Similarly, it is possible to use an independent  
571 measurement of binding potential at rest to substitute for either  $k_2$   
572 or  $k_{2a}$  to reduce the number of estimated parameters. (In MRTM,  $BP_{ND}$   
573 is given by  $(k_2/k_{2a}) - 1$ , which also holds in lp-ntPET for the binding  
574 potential of *baseline* data.) Thus the p-ntPET and lp-ntPET models are  
575 similar not only in their performance but also in their abilities to  
576 accommodate prior information.

#### 577 Magnitude of estimated responses

578 Like SRTM, lp-ntPET is based on a one-tissue compartment model.  
579 Neurotransmitter concentration is incorporated implicitly via time-  
580 varying change in  $k_{2a}$ , the rate of tracer efflux from the tissue  
581 compartment. In our simulations, which are based on an enhanced  
582 model that explicitly includes neurotransmitter concentration, the  
583 maximum receptor occupancy by released neurotransmitter was less  
584 than 30%. If we assume that neurotransmitter binding to receptors is  
585 instantaneous, the resulting increase in occupancy translates to an  
586 increase in apparent washout rate of 26%. This is in excellent  
587 agreement with the estimated peak values of  $k_{2a}(t)$  at ~30% above  
588 baseline (see Figs. 2–4).

589 We further note that the magnitude of neurotransmitter release  
590 examined in our simulations is physiologically plausible. Consider  
591 microdialysis findings following i.v. amphetamine administered to  
592 rhesus monkeys reported in Endres et al. (1997). Peak receptor  
593 occupancies by dopamine were estimated to be 52% and 62%  
594 following amphetamine doses of 0.2 mg/kg and 0.4 mg/kg, respec-  
595 tively. By comparison, we can classify our simulations based on 30%

peak occupancy and  $\Delta BP_{ND}$  less than 20% (Normandin and Morris, 596  
2008) as conservative. 597

#### Statistical detection of responses 598

599 Another difference between lp-ntPET and p-ntPET is the manner by  
600 which significant responses are detected. The p-ntPET model utilizes a  
601 threshold on the peak height of the estimated response to determine its  
602 significance. Here, we have evaluated a battery of statistical tests and  
603 model selection criteria to assess the significance of responses estimated  
604 by lp-ntPET. The p-ntPET model accurately classified responses for  
605 activation starting as late as 30 min (Normandin and Morris, 2008).  
606 Using model selection criteria and “uncorrected” statistical tests,  
607 lp-ntPET reliably detected true neurotransmitter responses starting  
608 as late as 35 to 40 min into the scan. “Corrected” statistical tests  
609 using Monte Carlo estimates of parameter variance were less  
610 sensitive to responses after 25 min (see Table 2). All detection  
611 methods showed high false discovery rates, particularly for dual-scan  
612 analyses with WLS optimization.

613 The false positive rates obtained for single-scan data sets also  
614 tended to be high but were in better agreement with the anticipated  
615 specificity based on the selected significance level ( $\alpha = 0.01$  in the  
616 simulation studies presented here). However, the responses estimat-  
617 ed from single-scan null data deviated from ideal behavior. The  
618 average magnitude across repeated simulations was biased toward  
619 positive values (Fig. 3D). While this was not a surprising finding for  
620 NNLS optimization, where decreases in neurotransmitter below  
621 baseline levels were not permitted, the behavior was not expected  
622 with WLS estimation. The same skewness toward positive  $\gamma$  values  
623 was not seen in analogous dual-scan data sets (see Figs. 2C, F and 3B),  
624 suggesting that the etiology of the phenomenon lies in the experiment  
625 design and not intrinsic model deficiencies. We hypothesize that  
626 without a complete rest scan the model cannot unambiguously  
627 distinguish tracer washout from neurotransmitter release. The use of  
628 a bolus-plus-infusion protocol to achieve steady-state might elimi-  
629 nate such transient confounds. The bolus-plus-infusion protocol could  
630 also provide a more uniform signal-to-noise ratio over the scan  
631 duration, reducing the time-dependence of sensitivity and specificity.  
632 Although we found activation-induced changes in blood flow to have  
633 minimal impact on the performance of lp-ntPET, the use of a bolus-  
634 plus-infusion protocol should further mitigate its impact (Carson  
635 et al., 1997). Bolus-plus-infusion administration of tracer for both rest  
636 and activation sessions might also increase the reliability of dual-scan  
637 analyses.

638 Application of lp-ntPET relies on significance testing to establish  
639 that  $\gamma$  is non-zero (i.e., fits are statistically better with a time-varying  
640 activation term than without). Each of the tests evaluated here has  
641 limitations in this application. One limitation is that the  $\gamma$  values  
642 estimated from null data sets do not conform to an unbiased Gaussian  
643 distribution. With WLS the model always invokes a non-zero response  
644 to reduce the sum of squares. With NNLS the non-negativity  
645 constraint imposes a positive bias. Hence uncorrected  $t$  and  $F$  tests  
646 are not for the analysis of null data and tend to exaggerate the  
647 significance of estimated responses. Corrected  $t$  and  $F$  tests using a  
648 Monte Carlo-derived estimate of parameter error do not correct the  
649 distribution of  $\gamma$  and cannot be readily applied to the analysis of  
650 experimental data sets. On the other hand, AIC and BIC rely on the  
651 quality of the model fit to the data. Results from these measures were  
652 in better agreement with theoretical expectations, although AIC and  
653 BIC still exhibited relatively high false positive rates (see Table 2). We  
654 posit that lp-ntPET sometimes invoked small responses to compen-  
655 sate for partial inadequacy of the underlying **simplified** model, as  
656 evidenced by WLS fits to null data which yield average estimated  
657 responses that are insubstantial but not identically zero (Figs. 2F  
658 and 3B,D). Of the significance tests investigated here, BIC showed the  
659 best combination of sensitivity and specificity. We therefore advise



using BIC with lp-ntPET. The NNLS optimization method generally had lower false positive rates using model selection tests than the WLS algorithm. NNLS is appropriate if it is known *a priori* whether neurotransmitter changes will increase or decrease. If such information is known in advance and the increased computation time (discussed in next section) is acceptable, NNLS is recommended as a more selective algorithm than WLS.

The generally unsatisfying performance of statistical tests for discrimination of significant responses warrants further examination. A hybrid analysis approach might utilize lp-ntPET to estimate neurotransmitter kinetics in combination with more conventional analysis methods such as binding potential for assessment of response significance.  $\Delta BP_{ND}$  is frequently used to detect changes in neurotransmitter levels between baseline and activation scan sessions. Although this method has known deficiencies for temporally variable responses in paired bolus experiments (Yoder et al., 2004),  $\Delta BP_{ND}$  is proportional to the integral of the neurotransmitter release profile in equilibrium studies (Endres and Carson, 1998). In addition to yielding steady-state conditions, bolus-plus-infusion tracer administration permits measurement of  $\Delta BP_{ND}$  in single-scan studies (Carson et al., 1997; Endres and Carson, 1998; Endres et al., 1997). Thus,  $\Delta BP_{ND}$  or other standard analyses could potentially be used to screen or mask data sets for detection of significant activation profiles estimated by lp-ntPET, even in single-scan experiments.

#### Computational efficiency

The most noteworthy difference between p-ntPET and lp-ntPET is in computational burden. p-ntPET relies on a compartmental model characterized by eleven parameters. Estimation of these parameters requires iterative, non-linear fitting. Because the fits exhibited some sensitivity to initial parameter guess, we fit each data set fifty times with different initial parameter values. The entire procedure takes approximately 60 to 90 minutes for a typical data set using the Levenberg–Marquardt algorithm on a standard computer workstation. lp-ntPET is based on a simplified compartmental model and has just four explicit parameters, all of which occur as linear coefficients in the operational equation. Although the model must be fitted to the data multiple times (once per basis function), each fit is very fast and requires iteration only if NNLS is used. Analysis of a typical dual-scan data set with a full catalog of response functions took less than 1.5 seconds using NNLS and less than 0.1 seconds using WLS. This represents a reduction in computation time of several orders of magnitude over p-ntPET with otherwise very similar performance.

The efficiency of lp-ntPET makes it practical to perform voxel-by-voxel analysis of the whole brain, an intractable task for p-ntPET. The resulting parametric images of  $\gamma$  could be processed using the well established framework of statistical parametric mapping (SPM; Friston et al., 1995) for detection of significant responses. In addition to facilitating statistical testing, the ability to perform parametric analysis with lp-ntPET would permit investigation of spatially and functionally heterogeneous responses or localized activation patterns that might be diluted using pre-defined regions of interest. Voxelwise analysis with lp-ntPET could produce informative visualizations, including 4D (3D in space, 1D in time) neurotransmitter “movies” or parametric images of key response parameters (e.g., time of peak neurotransmitter response), such as those generated from fMRI data (Marota et al., 2000) and recently demonstrated using results from non-parametric ntPET (Morris et al., 2010). These possibilities motivate ongoing work to evaluate the efficacy of denoising techniques (e.g., Alpert et al., 2006; Christian et al., 2010; Joshi et al., 2008; Zhou et al., 2003) and develop adaptations of lp-ntPET (such as constraining baseline  $BP_{ND}$  as described above, or using a global clearance rate for the reference region as in SRTM2 (Wu and Carson, 2002) and MRTM2 (Ichise et al., 2003)) to promote robust performance on noisy voxel-level data.

#### Conclusion

The lp-ntPET technique presented here is a basis function augmentation of the LSRRM method. LSRRM assumes that the time course of activation is known, and in particular, that the response onset coincides with task initiation. Our extension is more flexible. It permits temporal characterization of neurotransmitter fluctuations, including estimation of the response onset, peak time, and sharpness. Analysis of realistic simulated data demonstrated that the performance of lp-ntPET is similar to that of p-ntPET, which relies on an elaborate compartmental model to estimate the time course of neurotransmitter release. Computation time was several orders of magnitude faster using lp-ntPET. Simulation studies revealed that lp-ntPET is insensitive to anticipated model violations and may be applied to single-scan paradigms. Activation profiles estimated from PET data acquired in rats receiving methamphetamine were in good agreement with simultaneous microdialysis measurements of dopamine concentration. These results support the use of lp-ntPET as an efficient and practical technique for estimation of neurotransmitter dynamics from PET data.

#### Acknowledgments

M.D. Normandin acknowledges the support of the L.A. Geddes Fellowship and the Society of Nuclear Medicine Student Fellowship. E.D. Morris acknowledges the support of NIH grant R21 AA015077 and the Whitaker Foundation grants RG 02-0126 and TF 04-0034.

#### References

- Aalto, S., Brück, A., Laine, M., Nägren, K., Rinne, J.O., 2005. Frontal and temporal dopamine release during working memory and attention tasks in healthy humans: a positron emission tomography study using the high-affinity dopamine D2 receptor ligand [11C]FLB 457. *J. Neurosci.* 25, 2471–2477.
- Abi-Dargham, A., Gil, R., Krystal, J., Baldwin, R.M., Seibyl, J.P., Bowers, M., Van Dyck, C.H., Charney, D.S., Innis, R.B., Laruelle, M., 1998. Increased striatal dopamine transmission in schizophrenia: confirmation in a second cohort. *Am. J. Psychiatry* 155, 761–767.
- Akaike, H., 1974. A new look at the statistical model identification. *IEEE Trans. Autom. Control* 19, 716–723.
- Akaike, H., 1978. A Bayesian analysis of the minimum AIC procedure. *Ann. Inst. Stat. Math.* 30, 9–14.
- Alpert, N.M., Badgaiyan, R.D., Livni, E., Fischman, A.J., 2003. A novel method for noninvasive detection of neuromodulatory changes in specific neurotransmitter systems. *Neuroimage* 19, 1049–1060.
- Alpert, N.M., Reilhac, A., Chio, T.C., Seisenick, I., 2006. Optimization of dynamic measurement of receptor kinetics by wavelet denoising. *Neuroimage* 30, 444–451.
- Aston, J.A., Gunn, R.N., Worsley, K.J., Ma, Y., Evans, A.C., Dagher, A., 2000. A statistical method for the analysis of positron emission tomography neuroreceptor ligand data. *Neuroimage* 12, 245–256.
- Badgaiyan, R.D., Fischman, A.J., Alpert, N.M., 2003. Striatal dopamine release during unrewarded motor task in human volunteers. *Neuroreport* 14, 1421–1424.
- Badgaiyan, R.D., Fischman, A.J., Alpert, N.M., 2007. Striatal dopamine release in sequential learning. *Neuroimage* 38, 549–556.
- Badgaiyan, R.D., Fischman, A.J., Alpert, N.M., 2008. Explicit motor memory activates the striatal dopamine system. *Neuroreport* 19, 409–412.
- Breier, A., Su, T.P., Saunders, R., Carson, R.E., Kolachana, B.S., de Bartolomeis, A., Weinberger, D.R., Weisenfeld, N., Malhotra, A.K., Eckelman, W.C., Pickar, D., 1997. Schizophrenia is associated with elevated amphetamine-induced synaptic dopamine concentrations: evidence from a novel positron emission tomography method. *Proc. Natl. Acad. Sci.* 94, 2569–2574.
- Burnham, K.P., Anderson, D.R., 1998. *Model Selection and Inference: A Practical Information-Theoretic Approach*. Springer-Verlag, New York.
- Busto, U.E., Redden, L., Mayberg, H., Kapur, S., Zawertailo, L.A., 2009. Dopaminergic activity in depressed smokers: a positron emission tomography study. *Synapse* 63, 681–689.
- Carson, R.E., Breier, A., de Bartolomeis, A., Saunders, R.C., Su, T.P., Schmall, B., Der, M.G., Pickar, D., Eckelman, W.C., 1997. Quantification of amphetamine-induced changes in [11C]raclopride binding with continuous infusion. *J. Cereb. Blood Flow Metab.* 17, 437–447.
- Christian, B.T., Leher, D.S., Shi, B., Narayanan, T.K., Strohmeyer, P.S., Buchsbaum, M.S., Mantil, J.C., 2006. Measuring dopamine neuromodulation in the thalamus: using [F-18]fallypride PET to study dopamine release during a spatial attention task. *Neuroimage* 31, 139–152.
- Christian, B.T., Vandehey, N.T., Floberg, J.M., Mistretta, C.A., 2010. Dynamic PET denoising with HYPR processing. *J. Nucl. Med.* 51, 1147–1154.



- 795 Constantinescu, C.C., Bouman, C., Morris, E.D., 2007. Nonparametric extraction of  
796 transient changes in neurotransmitter concentration from dynamic PET data. *IEEE*  
797 *Trans. Med. Imaging* 26, 359–373.
- 798 Cox, S.M.L., Benkelfat, C., Dagher, A., Delaney, J.S., Durand, F., McKenzie, S.A., Koliavakis,  
799 T., Casey, K.F., Leyton, M., 2009. Striatal dopamine responses to intranasal cocaine  
800 self-administration in humans. *Biol. Psychiatry* 65, 846–850.
- 801 Cramér, H., 1946. *Mathematical Method of Statistics*. Princeton University Press.
- 802 de la Fuente-Fernández, R., Sossi, V., Huang, Z., Furtado, S., Lu, J.Q., Calne, D.B., Ruth, T.J.,  
803 Stoessl, A.J., 2004. Levodopa-induced changes in synaptic dopamine levels increase  
804 with progression of Parkinson's disease: implications for dyskinesias. *Brain* 127,  
805 2747–2754.
- 806 Endres, C.J., Carson, R.E., 1998. Assessment of dynamic neurotransmitter changes with  
807 bolus or infusion delivery of neuroreceptor ligands. *J. Cereb. Blood Flow Metab.* 18,  
808 1196–1210.
- 809 Endres, C.J., Kolachana, B.S., Saunders, R.C., Su, T., Weinberger, D., Breier, A., Eckelman,  
810 W.C., Carson, R.E., 1997. Kinetic modeling of [11C]raclopride: combined PET-  
811 microdialysis studies. *J. Cereb. Blood Flow Metab.* 17, 932–942.
- 812 Evans, A.H., Pavese, N., Lawrence, A.D., Tai, Y.F., Appel, S., Doder, M., Brooks, D.J., Lees,  
813 A.J., Piccini, P., 2006. Compulsive drug use linked to sensitized ventral striatal  
814 dopamine transmission. *Ann. Neurol.* 59, 852–858.
- 815 Fisher, R.A., 1925a. Applications of "Student's" distribution. *Metron* 5, 90–104.
- 816 Fisher, R.A., 1925b. *Statistical Methods for Research Workers*. Oliver and Boyd, Edinburgh.
- 817 Fried, I., Wilson, C.L., Morrow, J.W., Cameron, K.A., Behnke, E.D., Ackerson, L.C.,  
818 Maidment, N.T., 2001. Increased dopamine release in the human amygdala during  
819 performance of cognitive tasks. *Nat. Neurosci.* 4, 201–206.
- 820 Friston, K.J., Holmes, A.P., Worsley, K.J., Poline, J.P., Frith, C.D., Frackowiak, R.S.J., 1995.  
821 Statistical parametric maps in functional imaging: a general linear approach. *Hum.*  
822 *Brain Mapp.* 2, 189–210.
- 823 Friston, K., Malizia, A., Wilson, S., Cunningham, V., Jones, T., Nutt, D., 1997. Analysis of  
824 dynamic radioligand displacement or "activation" studies. *J. Cereb. Blood Flow*  
825 *Metab.* 17, 80–93.
- 826 Gosset [Student], W.S., 1908. The probable error of a mean. *Biometrika* 6, 1–25.
- 827 Gunn, R.N., Lammertsma, A.A., Hume, S.P., Cunningham, V.J., 1997. Parametric imaging  
828 of ligand-receptor binding in PET using a simplified reference region model.  
829 *Neuroimage* 6, 279–287.
- 830 Ichise, M., Liow, J.S., Lu, J.Q., Takano, A., Model, K., Toyama, H., Suhara, T., Suzuki, K.,  
831 Innis, R.B., Carson, R.E., 2003. Linearized reference tissue parametric imaging  
832 methods: application to [11C]DASB positron emission tomography studies of the  
833 serotonin transporter in human brain. *J. Cereb. Blood Flow Metab.* 23, 1096–1112.
- 834 Ikoma, Y., Watabe, H., Hayashi, T., Miyake, Y., Teramoto, N., Minato, K., Iida, H., 2009.  
835 Quantitative evaluation of changes in binding potential with a simplified reference  
836 tissue model and multiple injections of [11C]raclopride. *Neuroimage* 47, 1639–1648.
- 837 Innis, R.B., Cunningham, V.J., Delforge, J., Fujita, M., Gjedde, A., Gunn, R.N., Holden, J.,  
838 Houle, S., Huang, S.C., Ichise, M., Iida, H., Ito, H., Kimura, Y., Koeppe, R.A., Knudsen,  
839 G.M., Knuutti, J., Lammertsma, A.A., Laruelle, M., Logan, J., Maguire, R.P., Mintun,  
840 M.A., Morris, E.D., Parsey, R., Price, J.C., Slifstein, M., Sossi, V., Suhara, T., Votaw, J.R.,  
841 Wong, D.F., Carson, R.E., 2007. Consensus nomenclature for in vivo imaging of  
842 reversibly binding radioligands. *J. Cereb. Blood Flow Metab.* 27, 1533–1539.
- 843 Joshi, A., Fessler, J.A., Koeppe, R.A., 2008. Improving PET receptor binding estimates  
844 from Logan plots using principal component analysis. *J. Cereb. Blood Flow Metab.*  
845 *28*, 852–865.
- 846 Koeppe, M.J., Gunn, R.N., Lawrence, A.D., Cunningham, V.J., Dagher, A., Jones, T., Brooks,  
847 D.J., Bench, C.J., Grasby, P.M., 1998. Evidence for striatal dopamine release during a  
848 video game. *Nature* 393, 266–268.
- 849 Lammertsma, A.A., Hume, S.P., 1996. Simplified reference tissue model for PET receptor  
850 studies. *Neuroimage* 4, 153–158.
- 851 Landaw, E.M., DiStefano, J.J., 1984. Multiexponential, multicompartmental, and  
852 noncompartmental modeling. II. Data analysis and statistical considerations. *Am.*  
853 *J. Physiol.* 246, R665–R677.
- 854 Laruelle, M., Abi-dargham, A., Gil, R., Kegeles, L., Innis, R., 1999. Increased dopamine  
855 transmission in schizophrenia: relationship to illness phases. *Biol. Psychiatry* 46,  
856 56–72.
- 857 Madsen, M.T., 1992. A simplified formulation of the gamma variate function. *Phys. Med.*  
858 *Biol.* 37, 1597–1600.
- 859 Marota, J.J., Mandeville, J.B., Weisskoff, R.M., Moskowitz, M.A., Rosen, B.R., Kosofsky, B.E.,  
860 2000. Cocaine activation discriminates dopaminergic projections by temporal  
861 response: an fMRI study in rat. *Neuroimage* 11, 13–23.
- 862 Martinez, D., Gil, R., Slifstein, M., Hwang, D.R., Huang, Y., Perez, A., Kegeles, L., Talbot, P.,  
863 Evans, S., Krystal, J., Laruelle, M., Abi-Dargham, A., 2005. Alcohol dependence is  
864 associated with blunted dopamine transmission in the ventral striatum. *Biol.*  
865 *Psychiatry* 58, 779–786.
- 866 Martinez, D., Narendran, R., Foltin, R.W., Slifstein, M., Hwang, D.R., Broft, A., Huang, Y.,  
867 Cooper, T.B., Fischman, M.W., Kleber, H.D., Laruelle, M., 2007. Amphetamine-  
868 induced dopamine release: markedly blunted in cocaine dependence and  
869 predictive of the choice to self-administer cocaine. *Am. J. Psychiatry* 164, 622–629.
- 870 Mazoyer, B.M., Huesman, R.H., Budinger, T.F., Knittel, B.L., 1986. Dynamic PET data  
871 analysis. *J. Comput. Assist. Tomogr.* 10, 645–653.
- 872 Mintun, M.A., Raichle, M.E., Kilbourn, M.R., Wooten, G.F., Welch, M.J., 1984. A  
873 quantitative model for the in vivo assessment of drug binding sites with positron  
874 emission tomography. *Ann. Neurol.* 15, 217–227.
- 875 Morris, E.D., Fisher, R.E., Alpert, N.M., Rauch, S., Fischman, A.J., 1995. In vivo imaging of  
876 neuromodulation using positron emission tomography: optimal ligand character-  
877 istics and task length for detection of activation. *Hum. Brain Mapp.* 3, 35–55.
- 878 Morris, E.D., Yoder, K.K., Wang, C., Normandin, M.D., Zheng, Q.H., Mock, B., Muzic Jr.,  
879 R.F., Froehlich, J.C., 2005. ntPET: a new application of PET imaging for characterizing  
880 the kinetics of endogenous neurotransmitter release. *Mol. Imaging* 4, 473–489.
- 881 Morris, E.D., Normandin, M.D., Schiffer, W.K., 2008. Initial comparison of ntPET with  
882 microdialysis measurements of methamphetamine-induced dopamine release in  
883 rats: support for estimation of dopamine curves from PET data. *Mol. Imaging Biol.*  
884 *10*, 67–73.
- 885 Morris, E.D., Constantinescu, C.C., Sullivan, J.M., Normandin, M.D., Christopher, L.A.,  
886 2010. Noninvasive visualization of human dopamine dynamics from PET images.  
887 *Neuroimage* 51, 135–144.
- 888 Normandin, M.D., Morris, E.D., 2006. Temporal resolution of ntPET using either arterial  
889 or reference region-derived plasma input functions. *Conf. Proc. IEEE Eng. Med. Biol.*  
890 *Soc.* 1, 2005–2008.
- 891 Normandin, M.D., Morris, E.D., 2008. Estimating neurotransmitter kinetics with ntPET:  
892 a simulation study of temporal precision and effects of biased data. *Neuroimage* 39,  
893 1162–1179.
- 894 Olive, M.F., Nannini, M.A., Ou, C.J., Koenig, H.N., Hodge, C.W., 2002. Effects of acute  
895 acamprosate and homotaurine on ethanol intake and ethanol-stimulated meso-  
896 limbic dopamine release. *Eur. J. Pharmacol.* 437, 55–61.
- 897 Oswald, L.M., Wong, D.F., McCaul, M., Zhou, Y., Kuwabara, H., Choi, L., Brasic, J., Wand,  
898 G.S., 2005. Relationships among ventral striatal dopamine release, cortisol  
899 secretion, and subjective responses to amphetamine. *Neuropsychopharmacology*  
900 *30*, 821–832.
- 901 Oswald, L.M., Wong, D.F., Zhou, Y., Kumar, A., Brasic, J., Alexander, M., Ye, W., Kuwabara,  
902 H., Hilton, J., Wand, G.S., 2007. Impulsivity and chronic stress are associated with  
903 amphetamine-induced striatal dopamine release. *Neuroimage* 36, 153–166.
- 904 Pappata, S., Dehaene, S., Poline, J.B., Gregoire, M.C., Jobert, A., Delforge, J., Frouin, V.,  
905 Bottlaender, M., Dolle, F., Di Giambardino, L., Syrota, A., 2002. In vivo detection of  
906 striatal dopamine release during reward: a PET study with [11C]raclopride and a  
907 single dynamic scan approach. *Neuroimage* 16, 1015–1027.
- 908 Parasurampuria, D.A., Schoedel, K.A., Schuller, R., Gu, J., Ciccone, P., Silber, S.A., Sellers,  
909 E.M., 2007. Assessment of pharmacokinetics and pharmacodynamic effects related  
910 to abuse potential of a unique oral osmotic-controlled extended-release methyl-  
911 phenidate formulation in humans. *J. Clin. Pharmacol.* 47, 1476–1488.
- 912 Rao, C., 1945. Information and the accuracy attainable in the estimation of statistical  
913 parameters. *Bull. Calcutta Math. Soc.* 37, 81–89.
- 914 Sarter, M., Bruno, J., Parikh, V., 2007. Abnormal neurotransmitter release in behavioral  
915 and cognitive disorders: toward concepts of dynamic and function-specific  
916 dysregulation. *Neuropsychopharmacology* 32, 1452–1461.
- 917 Schwarz, G., 1978. Estimating the dimension of a model. *Ann. Stat.* 6, 461–464.
- 918 Spencer, T.J., Biederman, J., Ciccone, P.E., Madras, B.K., Dougherty, D.D., Bonab, A.A.,  
919 Livni, E., Parasurampuria, D.A., Fischman, A.J., 2006. PET study examining  
920 pharmacokinetics, detection and likeability, and dopamine transporter receptor  
921 occupancy of short- and long-acting oral methylphenidate. *Am. J. Psychiatry* 163,  
922 387–395.
- 923 Steeves, T.D.L., Miyasaki, J., Zurowski, M., Lang, A.E., Pelleccia, G., Van Eimeren, T.,  
924 Rusjan, P., Houle, S., Strafella, A.P., 2009. Increased striatal dopamine release in  
925 Parkinsonian patients with pathological gambling: a [11C]raclopride PET study.  
926 *Brain* 132, 1376–1385.
- 927 Volkow, N.D., Swanson, J.M., 2003. Variables that affect the clinical use and abuse of  
928 methylphenidate in the treatment of ADHD. *Am. J. Psychiatry* 160, 1909–1918.
- 929 Volkow, N.D., Mullani, N., Gould, L., Adler, S.S., Guynn, R.W., Overall, J.E., Dewey, S.,  
930 1988. Effects flow of acute measured alcohol intoxication with PET on cerebral  
931 blood. *New York J.* 24, 201–209.
- 932 Volkow, N.D., Ding, Y.S., Fowler, J.S., Wang, G.J., Logan, J., Gatley, J.S., Dewey, S., Ashby, C.,  
933 Liebermann, J., Hitzemann, R., Wolf, A.P., 1995. Is methylphenidate like cocaine?  
934 Studies on their pharmacokinetics and distribution in the human brain. *Arch. Gen.*  
935 *Psychiatry* 456–463.
- 936 Volkow, N.D., Ding, Y.S., Fowler, J.S., Wang, G.J., 1996. Cocaine addiction: hypothesis  
937 derived from imaging studies with PET. *J. Addict. Dis.* 15, 55–71.
- 938 Volkow, N.D., Wang, G.J., Fowler, J.S., Logan, J., Gatley, S.J., Hitzemann, R., Chen, A.D.,  
939 Dewey, S.L., Pappas, N., 1997. Decreased striatal dopaminergic responsiveness in  
940 detoxified cocaine-dependent subjects. *Nature* 386, 830–833.
- 941 Volkow, N.D., Wang, G.J., Fowler, J.S., Fischman, M., Foltin, R., Abumrad, N.N., Gatley, S.J.,  
942 Logan, J., Wong, C., Gifford, A., Ding, Y.S., Hitzemann, R., Pappas, N., 1999.  
943 Methylphenidate and cocaine have a similar in vivo potency to block dopamine  
944 transporters in the human brain. *Life Sci.* 65, PL7–PL12.
- 945 Volkow, N.D., Fowler, J.S., Wang, G.J., Ding, Y.S., Gatley, S.J., 2002. Role of dopamine in  
946 the therapeutic and reinforcing effects of methylphenidate in humans: results from  
947 imaging studies. *Eur. Neuropsychopharmacol.* 12, 557–566.
- 948 Wand, G.S., Oswald, L.M., McCaul, M.E., Wong, D.F., Johnson, E., Zhou, Y., Kuwabara, H.,  
949 Kumar, A., 2007. Association of amphetamine-induced striatal dopamine release  
950 and cortisol responses to psychological stress. *Neuropsychopharmacology* 32,  
951 2310–2320.
- 952 Watabe, H., Endres, C.J., Breier, A., Schmall, B., Eckelman, W.C., Carson, R.E., 2000.  
953 Measurement of dopamine release with continuous infusion of [11C]raclopride:  
954 optimization and signal-to-noise considerations. *J. Nucl. Med.* 41, 522–530.
- 955 Wu, Y., Carson, R.E., 2002. Noise reduction in the simplified reference tissue model for  
956 neuroreceptor functional imaging. *J. Cereb. Blood Flow Metab.* 22, 1440–1452.
- 957 Yoder, K.K., Wang, C., Morris, E.D., 2004. Change in binding potential as a quantitative  
958 index of neurotransmitter release is highly sensitive to relative timing and kinetics  
959 of the tracer and the endogenous ligand. *J. Nucl. Med.* 45, 903–911.
- 960 Zhou, Y., Endres, C.J., Brasic, J.R., Huang, S.C., Wong, D.F., 2003. Linear regression with  
961 spatial constraint to generate parametric images of ligand-receptor dynamic PET  
962 studies with a simplified reference tissue model. *Neuroimage* 18, 975–989.
- 963 Zhou, Y., Chen, M.K., Endres, C.J., Ye, W., Brasic, J.R., Alexander, M., Crabb, A.H., Guilarte,  
964 T.R., Wong, D.F., 2006. An extended simplified reference tissue model for the  
965 quantification of dynamic PET with amphetamine challenge. *Neuroimage* 33,  
966 550–563.